Neuron, Vol. 29, 73–84, January, 2001, Copyright ©2001 by Cell Press

Kinase-Dependent and Kinase-Independent Functions of EphA4 Receptors in Major Axon Tract Formation In Vivo

Klas Kullander,* Nicole K. Mather,† Francesca Diella,* Mirella Dottori,‡ Andrew W. Boyd,‡ and Rüdiger Klein*§
*European Molecular Biology Laboratory
Meyerhofstrasse 1
D-69117 Heidelberg
Germany
†Department of Human Anatomy and Genetics
South Park Road
Oxford, OX1 3QX
United Kingdom
‡Queensland Institute for Medical Research
Royal Brisbane Hospital
Herston, Queensland 4029
Australia

Summary

The EphA4 receptor tyrosine kinase regulates the formation of the corticospinal tract (CST), a pathway controlling voluntary movements, and of the anterior commissure (AC), connecting the neocortical temporal lobes. To study EphA4 kinase signaling in these processes, we generated mice expressing mutant EphA4 receptors either lacking kinase activity or with severely downregulated kinase activity. We demonstrate that EphA4 is required for CST formation as a receptor for which it requires an active kinase domain. In contrast, the formation of the AC is rescued by kinase-dead EphA4, suggesting that in this structure EphA4 acts as a ligand for which its kinase activity is not required. Unexpectedly, the cytoplasmic sterile-alpha motif (SAM) domain is not required for EphA4 functions. Our findings establish both kinase-dependent and kinase-independent functions of EphA4 in the formation of major axon tracts.

Introduction

The development of the vertebrate nervous system involves many different morphogenetic processes, including organized and directed cell movements, the establishment of compartment boundaries, the generation and guidance of axons, the formation of topographically ordered neuronal networks and synaptogenesis. All of these processes involve communication between cells either at a distance or mediated by contact. The latter is achieved to a large extend by a family of cell surface proteins, termed ephrins, and their receptors, the Eph tyrosine kinases (reviewed in Flanagan and Vanderhaeghen, 1998; Holder and Klein, 1999; O'Leary and Wilkinson, 1999). Ephrins belong to the subclass of repulsive guidance cues, i.e., Eph receptor–expressing axons will migrate away from ephrin-expressing cells. Likewise, Eph receptor–expressing migratory cells will not intermingle with ephrin-expressing cells but rather try to minimize contact, thereby establishing sharp compartment boundaries (reviewed in Klein, 1999; Wilkinson, 2000).

The vertebrate genome contains at least 14 different *eph* genes, which are subdivided into two structurally distinct subclasses, termed *ephA1* through *ephA8* and *ephB1* through *ephB6*. The encoded receptors also differ in their ligand binding specificities. EphA receptors bind to ephrinA ligands, which are glycosylphosphatidylinositol-anchored proteins, whereas EphB receptors bind to ephrinB ligands, which are transmembrane proteins carrying a highly conserved 80 amino acid cytoplasmic domain. Whereas binding within a subgroup is promiscuous, little cross binding between the two subclasses has been observed. The EphA4 receptor is an exception to this rule in that it binds several ephrinA ligands, as well as the transmembrane ligands ephrinB2 and ephrinB3 (Wilkinson, 2000).

A distinctive feature of the ephrin/Eph ligand/receptor system is that signals can be transduced bidirectionally (Holder and Klein, 1999; Wilkinson, 2000). Binding of ephrins to Eph receptors activates their tyrosine-specific kinase domain and triggers intracellular signaling in the cells expressing the Eph receptor. Stimulation of ephrinB-expressing cells with the soluble EphB receptor ectodomain fused to the Fc portion of human IgG (EphB-Fc) causes rapid tyrosine phosphorylation of the ephrinB cytoplasmic domain, suggesting that ephrinB ligands also have receptor-like functions (Holland et al., 1996; Brückner et al., 1997). Genetic studies in mice and *C. elegans* showed that Eph receptors can have kinase-independent functions (Henkemeyer et al., 1996; Chin-Sang et al., 1999; Wang et al., 1999; Birgbauer et al., 2000), and cell sorting in the zebrafish hindbrain can be induced by C-terminally truncated Ephs, suggesting "reverse" signaling by ephrinB ligands (Xu et al., 1999).

A number of *ephrin* and *eph* gene knockouts in mice have revealed critical functions of this ligand/receptor family in the formation of topographic networks in the visual system, of commissural projections between left and right brain hemispheres, and in the developing vasculature (Henkemeyer et al., 1996; Orioli et al., 1996; Park et al., 1997; Wang et al., 1998; Adams et al., 1999; Gerety et al., 1999; Feldheim et al., 2000; Feng et al., 2000). Despite the rapid progress in understanding biological functions of ephrins and Ephs, the elucidation of the mechanism of signaling has proven difficult. In many tissues, ligands and receptors are coexpressed and have multiple binding partners (Flanagan and Vanderhaeghen, 1998; Adams et al., 1999; Hornberger et al., 1999), Moreover, "reverse" signaling by ephrins adds complexity to the system, since the direction of signaling could go three ways: unidirectional via forward signaling of Ephs, unidirectional via reverse signaling of ephrins, or bidirectional via both Ephs and ephrins (reviewed in Brückner and Klein, 1998; Holland et al., 1998; Wilkinson, 2000). In particular, the role of the Eph kinase domain in axon guidance has not been resolved using genetics. EphA receptors expressed on retinal ganglion cell axons

§To whom correspondence should be addressed (e-mail: klein@embl-heidelberg.de).

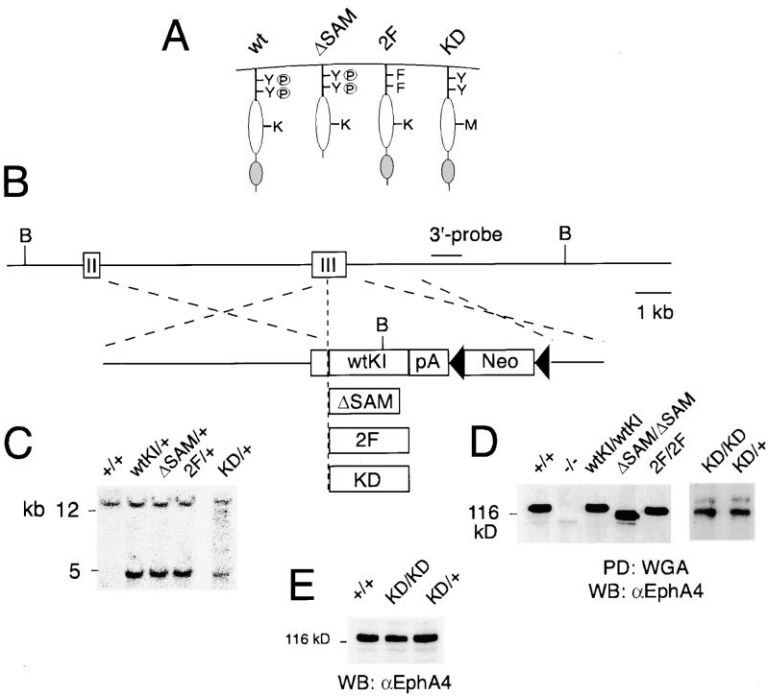

Figure 1. Generation of *ephA4* cDNA Knockin Mutants

(A) Schematic models of the intracellular parts of wild-type (wt) and mutant EphA4 proteins. We produced mutated cDNAs that encoded kinase-dead (KD) EphA4 with lysine residue K653 in the small lobe of the kinase domain (white oval) replaced by methionine, EphA4 with juxtamembrane tyrosine residues Y596 and Y604 (-Y-P) replaced by phenylalanines (2F), and EphA4 lacking the entire the SAM domain (gray oval) (Δ*SAM*).

(B) Schematic representation of the mouse *ephA4* gene used for the recombination strategy. Replacement-type vectors containing either wild-type (wtKI) or mutated cDNAs (see [A]) were fused in-frame with the third exon (III) and thereby placed under control of the endogenous gene promoter. A loxP-flanked (black triangles) neomycin selection marker was used for subsequent removal by the Cre recombinase. BamHI restriction sites (B) and location of the Southern hybridization probe are indicated.

(C) Homologous recombination was verified by Southern hybridization with ES cell genomic DNA following enzymatic restriction by BamHI. The probe corresponded to intronic sequences adjacent to the 3′ end of the targeted region (see [B]) and detected a 12.5 kb wild-type (+/+) and a 4.6 kb targeted DNA fragment in clones of transfected, heterozygous *ephA4*^{wtKI} (wtKI/+), *ephA4*$^{\Delta SAM}$ (ΔSAM/+), *ephA4*^{2F} (2F/+), or *ephA4*^{KD} (KD/+) ES cells.

(D) EphA4 protein levels in homozygous wild-type (+/+), null mutant (−/−), and knockin mutants (as indicated) determined by wheat germ agglutinin (WGA) pull-downs (PD) from adult brain extracts followed by immunoblotting (WB) of the EphA4 C terminus using an EphA4-specific antibody. Adult (left panel) and P14 (right panel) brains were used. Note the faster migration of the EphA4$^{\Delta SAM}$ protein. Levels of cDNA encoded EphA4 proteins were found to be equal to wild-type levels in the presence and absence (data not shown) of the *neo* cassette. Thus, most of the data in this study were generated using *ephA4*/*neo*$^{+}$ alleles and certain experiments were confirmed with *ephA4*/*neo*$^{-}$/*cre*$^{-}$ alleles (see text).

(E) EphA4 immunoblots of whole tissue lysates showing equal protein levels in +/+, homozygous, and heterozygous *ephA4*^{KD} mutant brains from newborn (P2) animals (similar results were obtained with other *ephA4* mutants).

are thought to mediate the formation of topographic projections to their targets in the brain (Flanagan and Vanderhaeghen, 1998; O'Leary and Wilkinson, 1999; Brown et al., 2000). However, it remains to be investigated if Eph receptors require catalytic activity to drive this process. Targeted knockin of a truncated EphB2 receptor, which was catalytically inactive and lacked most cytoplasmic sites of protein–protein interactions, rescued anterior commissure formation and retinal ganglion cell pathfinding, suggesting that EphB2 has predominantly, if not exclusively, kinase-independent functions in axon guidance (Henkemeyer et al., 1996; Birgbauer et al., 2000). The EphB2 cytoplasmic domain was rather required for vestibular fluid regulation, whereas minor pathfinding errors in this system were transient and compensated by other Eph receptors (Cowan et al., 2000).

The signal transduction events triggered by activated Eph receptors are complex and not well understood. The Eph cytoplasmic region is subdivided into four separate entities, each with its own signaling potential. The juxtamembrane region contains two conserved tyrosine residues, which are major autophosphorylation sites and, when phosphorylated, constitute docking sites for multiple SH2 domain–containing effectors (Brückner and Klein, 1998; Kalo and Pasquale, 1999). The tyrosine kinase domain provides catalytic activity and may itself be a binding site for adaptor proteins. Unique to this receptor family is a potential dimerization domain, termed sterile-α motif (SAM) domain, which upon autophosphorylation interacts with a distinct set of proteins. The three-dimensional structure of the Eph SAM domain suggests a role in the formation of higher order receptor clusters (Smalla et al., 1999; Stapleton et al., 1999; Thanos et al., 1999). The C-terminal tail of most Eph receptors carries a PDZ domain target site, which is able to recruit several PDZ domain–containing proteins, which may have roles in targeting receptors to subcellular sites, in receptor clustering or signaling (Hock et al., 1998; Torres et al., 1998; Brückner et al., 1999; Buchert et al., 1999; Lin et al., 1999).

In this study, we analyzed the mechanism of EphA4 signaling in axon tract formation during mouse neural development. Previously, *ephA4* null mutant mice were shown to have defects in the corticospinal tract (CST), a major motor pathway that controls voluntary movements. The apparent absence of ephA4 expression in the CST suggested a non-cell-autonomous role of EphA4 in this system (Dottori et al., 1998). Furthermore, the anterior commissure (AC), a large forebrain axon tract, failed to form in *ephA4* null mutants. Using knockin mutagenesis in mice, we now show that, contrary to a previous report, EphA4 exerts a cell-autonomous role in CST formation and requires a catalytically active kinase

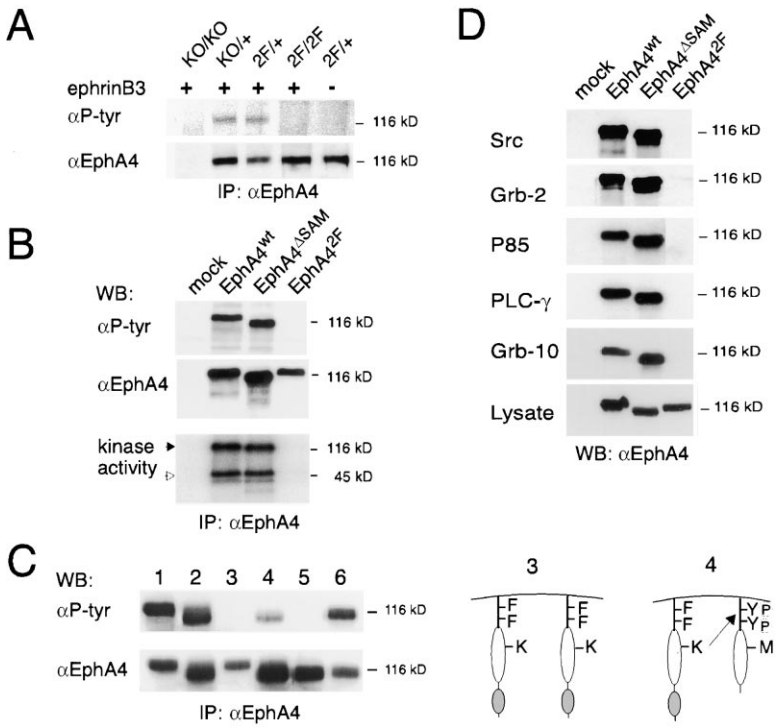

Figure 2. Mutation of Two Juxtamembrane Tyrosines in EphA4 Results in a Kinase-Deficient Receptor

(A) Dissociated E15.5 cortical neurons derived from either homozygous or heterozygous *ephA4*^{KO} and *ephA4*^{2F} mice were either left unstimulated (−) or were stimulated for 10 min with soluble ephrinB3-Fc. Anti-EphA4 immunoprecipitates were analyzed by immunoblotting with anti-phosphotyrosine antibodies to visualize EphA4 autophosphorylation (upper panel) or with anti-EphA4 antibodies to visualize EphA4 protein levels (lower panel). EphA4 receptors in neurons derived from heterozygotes were autophosphorylated (lanes 2 and 3), whereas no EphA4 autophosphorylation could be detected in *ephA4*$^{KO/KO}$- or *ephA4*$^{2F/2F}$-derived cortical cultures (lanes 1 and 4).

(B) Kinase activity of EphA4 overexpressed in 293 cells. Wild-type and mutant EphA4 proteins were immunoprecipitated from lysates of transfected 293 cells using anti-EphA4 antiserum and immunoblotted with anti-phosphotyrosine antibodies (upper panel). The blot was reprobed with anti-EphA4 antiserum to determine protein levels (middle panel). To analyze kinase activity of mutant EphA4 receptors, we performed in vitro kinase assays on anti-EphA4 immunoprecipitates in the presence of ^{32}P-γATP and enolase as exogenous substrate. After SDS–PAGE and exposure to x-ray film, we detected ^{32}P-labeled autophosphorylated EphA4 (black arrowhead) and enolase (open arrowhead; lower panel). Upon longer exposure of the film, low levels of phosphorylated enolase could be detected in EphA4^{2F}-expressing cells (data not shown).

(C) In cotransfection experiments, EphA4^{2F} protein phosphorylated a kinase-dead version of EphA4 (see model on the right). Lanes (1) wild-type EphA4 alone (EphA4^{WT}), (2) EphA4^{WT} plus kinase-dead EphA4$^{\Delta SAM}$ (EphA4$^{KD\Delta SAM}$), (3) EphA4^{2F} alone, (4) EphA4^{2F} plus EphA4$^{KD\Delta SAM}$, (5) EphA4$^{KD\Delta SAM}$ alone, (6) kinase active EphA4$^{\Delta SAM}$ alone. Constructs were cotransfected in 293 cells, immunoprecipitated using anti-EphA4 antiserum, separated by SDS–PAGE, immunoblotted with anti-phosphotyrosine antibodies (upper panel), and reprobed with anti-EphA4 antiserum to determine protein levels (lower panel). Note that EphA4^{2F} receptors fail to autophosphorylate (lane 3), but transphosphorylate kinase-dead EphA4$^{KD\Delta SAM}$ on juxtamembrane residues (lane 4).

(D) GST fusion proteins of the indicated SH2 domains and full-length Grb2 were immobilized on glutathione sepharose beads and incubated with lysates from 293 cells transfected with the indicated EphA4 mutants. Pull-downs were washed, run in 7.5% SDS–PAGE, and immunoblotted with anti-EphA4 antiserum. Anti-EphA4 immunoblots of whole-cell lysates showed similar expression levels of transfected cDNAs and absence of EphA4 in control vector transfectants (mock; lower panel).

domain. In contrast, EphA4 mediates guidance of AC axons in the absence of intrinsic kinase activity. In this structure, EphA4 presumably acts as a ligand for ephrins expressed on commissural axons. The conserved SAM domain is not required for EphA4-mediated axon guidance, neither for EphA4 kinase signaling, nor for its kinase-independent function as a ligand. Our findings demonstrate a requirement for both kinase-dependent and kinase-independent functions of EphA4 in the formation of major axon tracts.

Results

Generation of Mutant Mice Expressing Signaling-Deficient EphA4

We generated a series of *ephA4* mutants by targeted insertion (knockin) of cDNAs encoding either wild-type control EphA4 (*ephA4*^{wtKI}) or kinase-dead EphA4 (*ephA4*^{KD}). We further addressed the role of two conserved tyrosine residues in the juxtamembrane region of EphA4 by mutating both tyrosines to phenylalanine (*ephA4*^{2F}). Finally, we deleted the conserved SAM domain (*ephA4*$^{\Delta SAM}$), to investigate the requirement of this domain in EphA4 signaling and clustering. The *ephA4*$^{\Delta SAM}$ mutation left intact the carboxyterminal PDZ target site. (Figures 1A and 1B). To control for correct engineering of the knockin alleles, we performed Southern analysis of the targeted ES cells (Figure 1C) and we investigated EphA4 expression in homozygous mutant brains by Western blot analysis. We visualized fully matured, glycosylated EphA4 by pull-down experiments using wheat germ agglutinin (WGA), a lectin that binds to N-acetyl-β-D-glucosamyl residues of glycosylated cell surface proteins, followed by anti-EphA4 immunoblotting. Brain lysates from all knockin mutants, regardless of the presence or absence of the *neo* selection cassette (data not shown), expressed equal amounts of EphA4 protein at levels well comparable to wild-type brains (Figure 1D). Immunoblotting EphA4 from total cell lysates of newborn brains gave the same results, confirming that WGA pull-downs were quantitative and that EphA4 expression was high throughout postnatal development (Figure 1E).

Juxtamembrane Tyrosine Residues Regulate EphA4 Tyrosine Kinase Activity in Cortical Neurons

We next analyzed EphA4 receptor activation in primary cultures of embryonic (E15.5) cortical neurons, stimu-

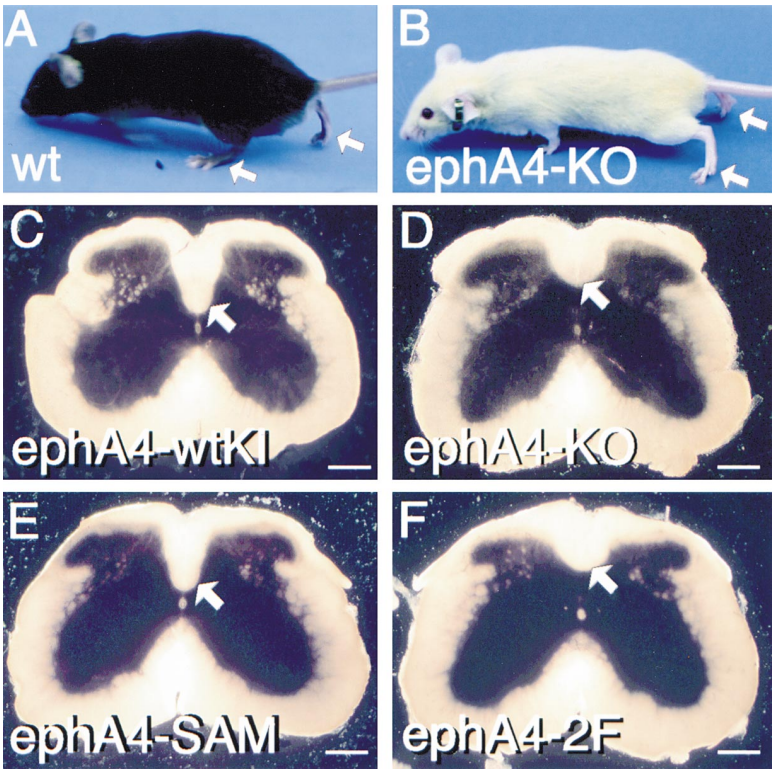

Figure 3. Motor Deficits and Spinal Cord Malformations of *ephA4* Mutant Mice

(A and B) Mice photographed during normal locomotion. (A) Wild-type mice run with normal rhythmically alternating hindlimbs (white arrows), whereas (B) *ephA4*^{KO} mice run with parallel hindlimbs similar to rabbits. Note the parallel extension of hindlimbs as the mouse is moving forward.

(C–F) DAB stains of 100 μm cryo-sections of the lumbar spinal cord. The ventral part of the dorsal funiculus (white arrow), where CST fibers are located, is normal in homozygous (C) control *ephA4*^{wtKI} and (E) *ephA4*$^{\Delta SAM}$ mice, whereas this structure is greatly reduced in (D) *ephA4*^{KO}, in (F) *ephA4*^{2F}, and in *ephA4*^{KD} mice (data not shown).

Scale bars: 200 μm.

lated with soluble ephrinB3 ligand ectodomain fused to the Fc portion of human IgG (ephrinB3-Fc). While neurons derived from *ephA4* homozygous null mutants (KO/KO) did not give a signal in this assay, autophosphorylated EphA4 receptors were seen in heterozygous mutants (KO/+) and in neurons derived from homozygous *ephA4*^{wtKI} and *ephA4*$^{\Delta SAM}$ alleles (Figure 2A and data not shown). In contrast, EphA4 in neurons derived from homozygous *ephA4*^{2F} mutants was not autophosphorylated (Figure 2A). Similar results were obtained using ephrinA3-Fc as stimulating ligand (data not shown). These findings indicated that the two juxtamembrane tyrosine residues somehow regulated EphA4 tyrosine kinase activity in cortical neurons, similar to recently published findings in cell lines ectopically expressing EphB2 or EphA4 receptors (Binns et al., 2000; Zisch et al., 2000).

To analyze the signaling potential of EphA4$^{\Delta SAM}$ and EphA4^{2F} receptors, we performed kinase assays on EphA4 mutant receptors expressed in HEK293 cells. In this cell system, EphA4 receptors are overexpressed and constitutively autophosphorylated in the absence of exogenous ephrin ligands (Figure 2B). Under these conditions, EphA4^{2F} receptors were not autophosphorylated and displayed greatly reduced kinase activity toward an exogenously added substrate such as enolase (Figure 2B). In contrast, deletion of the SAM domain did not impair receptor autophosphorylation and substrate phosphorylation (Figure 2B). To investigate if EphA4^{2F} receptors could phosphorylate other Eph receptors at juxtamembrane tyrosine residues, we coexpressed mutant EphA4^{2F} receptors with an EphA4 receptor carrying both juxtamembrane tyrosine residues. This EphA4 "substrate" was made kinase inactive to measure EphA4^{2F} kinase activity and, in addition, lacked the SAM domain to allow identification by size in Western blots. As shown in Figure 2C, lanes 3 and 5, separate expression of EphA4^{2F} receptors and kinase inactive EphA4 substrate did not yield any tyrosine-phosphorylated signal. In contrast, coexpression of EphA4^{2F} receptors and kinase inactive EphA4 substrate resulted in reduced but detectable expression of tyrosine-phosphorylated EphA4 substrate (Figure 2C, lane 4), indicating that EphA4^{2F} receptors were still capable of transphosphorylating juxtamembrane tyrosine residues of coexpressed EphA4 receptors.

We next performed pull-down experiments with SH2 domains of putative substrates of EphA4. SH2 domains of Src tyrosine kinase, p85 phosphatidylinositol-3′ kinase (p85 PI3K), phospholipase Cγ (PLCγ), Grb10 adaptor, as well as full-length Grb2 adaptor, all pulled down wild-type and EphA4$^{\Delta SAM}$ but not EphA4^{2F} receptors from 293 cell lysates (Figure 2D). Together, our biochemical analysis demonstrated the successful knockin of three EphA4 mutants, whose activities range from catalytically inactive (EphA4^{KD}) to severely compromised (EphA4^{2F}) to fully active (EphA4$^{\Delta SAM}$), at least under in vitro conditions.

EphA4 Kinase Signaling Is Required for Corticospinal Tract Formation

We next asked if any of the *ephA4* receptor mutants would resemble the *ephA4* null phenotype that is characterized by a parallel-hopping gait due to lack of hindbrain locomotor coordination and aberrant termination patterns of CST axons in brainstem and spinal cord (Dottori et al., 1998). Similar results were reported in an independently generated *ephA4* knockout in addition to defects in limb motor axon pathfinding (Helmbacher et

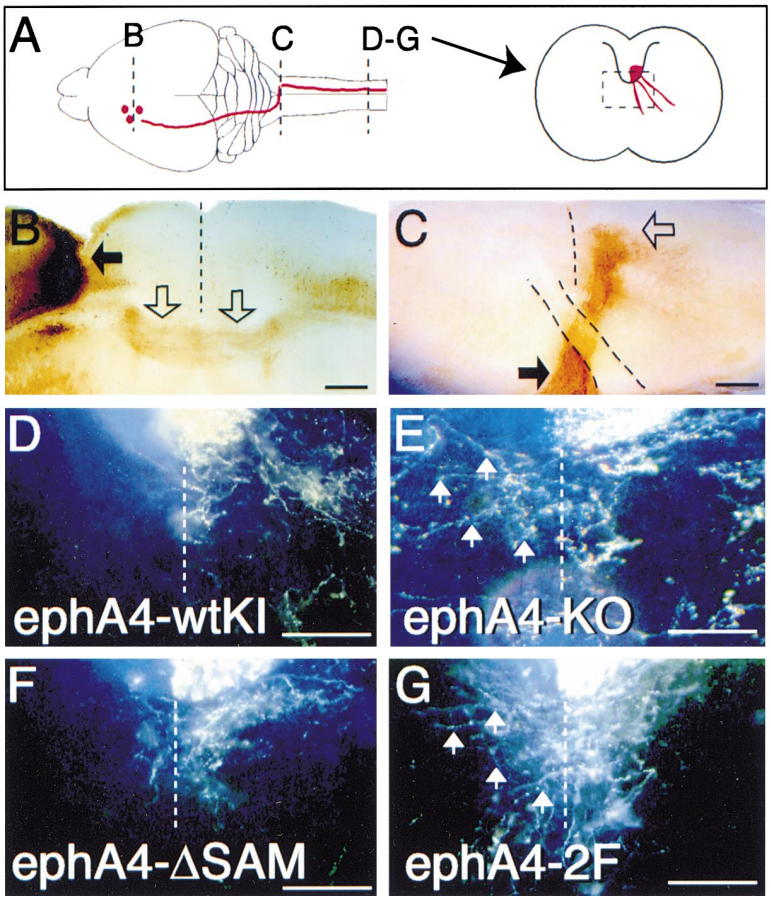

Figure 4. Aberrant Midline Recrossing of Corticospinal Tract Fibers in *ephA4* Mutant Mice

(A) Schematic drawing (anterior left), depicting the sites of tracer injection (red dots) and the path of the CST (red line) from the somatomotor cortex (B), via the medullary decussation (C) into the spinal cord (D–G). Coronal sections were taken as indicated (left drawing) and the stippled black box in the right drawing shows the area depicted in (D)–(G).

(B) Coronal section showing a neuronal tracer injected unilaterally in the somatomotor cortex. The site of injection is indicated with a black arrow and open arrows point to labeled corpus callosum fibers. The midline is indicated by a stippled line.

(C) Coronal section at the level of the medullary decussation, confirming unilateral labeling of the CST. The CST not only crosses the midline but also shifts from ventral (black arrow) to dorsal (open arrow). The contralateral unlabeled CST is indicated by stippled lines.

(D–G) CST fibers were unilaterally labeled (right) and were only occasionally seen to recross the midline in the thoracolumbar part of the spinal cord in (D) *ephA4*^{wtKI} and (F) *ephA4*$^{\Delta SAM}$ mice. In contrast, many CST fibers (white arrows) recrossed the midline in (E) *ephA4*^{KO}, (G) *ephA4*^{2F}, and *ephA4*^{KD} mice (data not shown).

Scale bars: 200 μm in (B), (C), 70 μm in panels (D)–(G).

al., 2000). Because EphA4 was thought to act non-cell autonomously as a ligand for ephrinB3-expressing CST axons (Dottori et al., 1998), we expected that kinase-dead EphA4 would rescue the CST defect. However, mice expressing either kinase-dead EphA4 or the severe EphA4^{2F} signaling mutant receptor suffered from the same parallel hopping gait hindlimb phenotype as *ephA4* null mutants (Figures 3A and 3B, and Videos 1 and 2 [http://www.neuron.org/cgi/content/full/29/1/73/DC1]). The presence or absence of the *neo* selection marker did not change this phenotype (data not shown). In contrast, control *ephA4*^{wtKI} and all heterozygous mutants displayed normal locomotion with alternating, independently moving hindlimbs (data not shown).

Histological analysis of spinal cord cross-sections of *ephA4*^{KD} (data not shown) and *ephA4*^{2F} homozygotes revealed reductions of white matter in the dorsal funiculus of the spinal cord, most prominently at lumbar levels, similar to *ephA4* null mutants (Figures 3D and 3F). In contrast, homozygous mice carrying the control *ephA4*^{wtKI} allele and all heterozygous mutants had a normally shaped dorsal funiculus (Figure 3C and data not shown). To visualize CST axons, we performed unilateral, anterograde axon tracing experiments in the somatomotor cortex and stained the terminal projections of the CST in the spinal cord (Figure 4A). To ascertain proper unilateral labeling, we examined the injection site (Figure 4B) and the medullary decussation (Figure 4C) for all animals (n = 3 for each genotype). We did not observe aberrant CST axons at the level of the medullary decussation. At lumbar level, we observed many aberrant axon sprouts in *ephA4* null and *ephA4*^{2F} mutants. Axons that descended in the dorsal funiculus contralateral to the tracer injection side were found to recross the midline (to the left) and to terminate ipsilateral to the injection side (Figures 4E and 4G; see also Dottori et al., 1998). Such aberrant projections were only rarely observed in wild-type (data not shown) or control *ephA4*^{wtKI} mice (Figure 3D). Our genetic analysis therefore indicated that EphA4 kinase activity is required for CST formation and hindlimb locomotor coordination in mice.

To identify the cells in which EphA4 signaling is required, we reexamined the expression pattern of EphA4 and candidate ephrin ligands in somatomotor cortex, brainstem, and spinal cord. In situ hybridization analysis of E15.5 somatomotor cortex revealed numerous ephA4-positive cells in the cortical plate and ventricular zone (Figure 5A). Similar to a previous report (Dottori et al., 1998), ephrinB3, one of the potential ligands of EphA4, was expressed in cortical plate, intermediate, and subventricular zones of the somatomotor cortex, albeit at low levels (Figure 5C). In contrast, ephrinB2, the only other ephrinB ligand shown to interact with EphA4 (Gale et al., 1996; Mellitzer et al., 1999) was absent from cortical plate at this stage of development and was largely confined to subventricular and ventricular

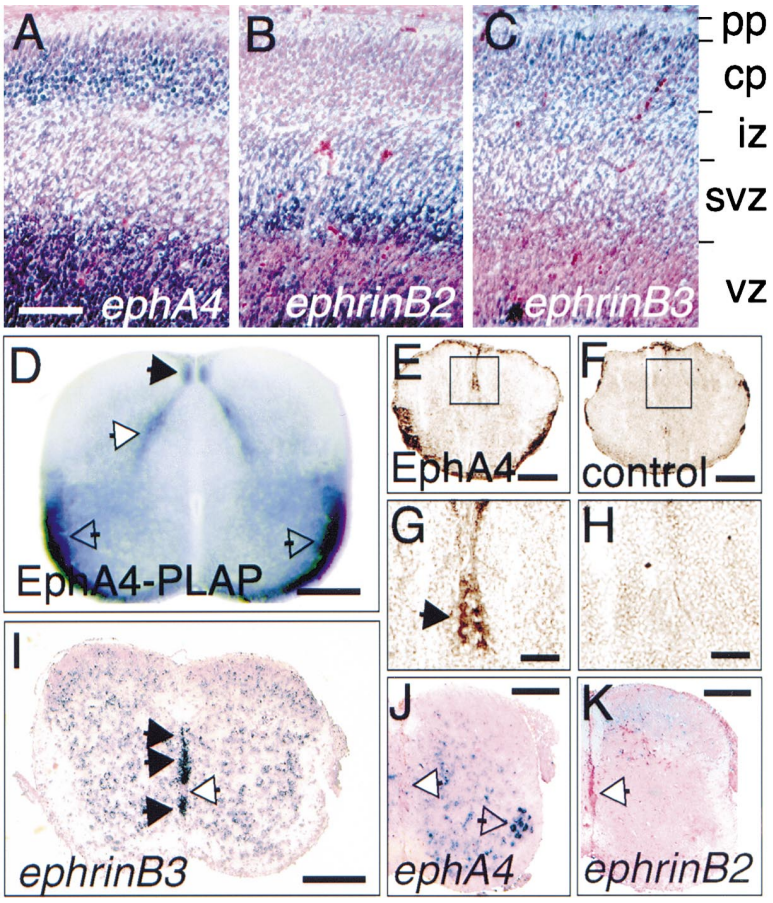

Figure 5. EphA4 Is Expressed in Somatomotor Cortex and in the Dorsal Funiculus

(A–C) Sagittal sections of E15.5 somatomotor cortex processed with DIG in situ hybridization using antisense probes for ephA4, ephrinB2, ephrinB3, respectively (blue staining), and counterstained with eosin (pink staining). Abbreviations: PP, primordial plexiform layer; CP, cortical plate; IZ, intermediate zone; SVZ, subventricular zone; VZ, ventricular zone. Note expression of ephA4 mRNA in cortical plate and ventricular zone.

(D) Transverse section of postnatal day 4 lumbar spinal cord from an EphA4 heterozygous gene trap mouse stained for PLAP activity. PLAP histochemistry reveals EphA4 expression in the descending corticospinal tract axons in the dorsal funiculus (arrow) and in their collateral branches (white arrow) that project into the gray matter of the spinal cord. PLAP histochemistry reveals EphA4 expression in other areas of the spinal cord in addition to the CST (open arrow). See Leighton et al. (2001) for details.

(E–H) EphA4 immunostaining (E and G) and preimmune control staining (F and H) of postnatal day 1 cervical spinal cord. Note strongest EphA4 immunoreactivity in the ventral aspects of the dorsal funiculus, where CST axons are located (arrow) (G).

(I–K) Postnatal day 4 spinal cord section hybridized with antisense probes as indicated. Note intense staining in the midline (black arrows) ventral to the dorsal funiculus and dorsal and ventral of the central canal (white arrow) (I). No midline stain was observed using ephA4 or ephrinB2 probes (J and K). Note positive ephA4 staining of motoneuron population in J (open arrow).

Scale bars: 120 μm in (A)–(C); 200 μm in (D)–(F) and (I)–(K); and 70 μm in (G) and (H).

zones (Figure 5B). We next visualized EphA4 protein by immunostaining of lumbar spinal cord section using an anti-EphA4-specific antiserum. We found specific staining in the ventral aspects of the dorsal funiculus, exactly where longitudinal CST axon bundles are located in rodents (Joosten and Bär, 1999) (Figures 5E–5H). Moreover, a novel *ephA4* gene trap mouse, in which placental alkaline phosphatase expression is controlled by ephA4 regulatory elements, demonstrated specific staining in the dorsal funiculus and descending fibers (Figure 5D; see also Leighton et al., 2001). This expression pattern of EphA4 in CST neurons together with abnormal CST projections in mice expressing signaling deficient EphA4, indicate a cell-autonomous receptor-like function of EphA4 in CST development. Whether or not a population of cells in the cortical plate of the motor cortex coexpresses EphA4 and ephrinB3 ligand remains to be established. We next examined the expression pattern of EphA4 and two candidate ligands, ephrinB2 and ephrinB3, in the spinal cord at postnatal day 4 when CST fibers are approaching. Based on the presence of ephrinB3 and absence of ephA4 and ephrinB2 expression in the spinal cord midline (Figure 5I–5K and Imondi et al., 2000), we suggest that in wild-type animals ephrinB3 may be preventing EphA4-expressing CST axons from recrossing the midline (see below).

The SAM Domain Is Dispensable for EphA4 Signaling in CST Axons

Having established an essential function for EphA4 tyrosine kinase activity in CST formation in vivo, we next asked whether the presence of the conserved SAM domain in the cytoplasmic tail of EphA4 was required in this process. Based on the tendency of isolated SAM domains to form dimers and oligomers (Smalla et al., 1999; Stapleton et al., 1999; Thanos et al., 1999), we expected that the presence of the SAM domain was necessary for Eph receptor signaling in vivo. Surprisingly, homozygous mutants that carried the *ephA4*$^{\Delta SAM}$ allele showed alternating and independent movements of the hindlimbs typical for wild-type control mice (Video 3 [http://www.neuron.org/cgi/content/full/29/1/73/DC1]). Their spinal cords were endowed with a normally shaped dorsal funiculus (Figure 3E) and showed normal terminal projections of anterogradely labeled CST axons, indistinguishable from wild-type control mice (Figure 4F). These results demonstrate that the presence of the SAM domain in EphA4 is not required for EphA4-mediated development of the CST.

Expression of EphA4 and EphrinB2 in the Forebrain

A previous report had indicated a requirement for EphA4 in the formation of the anterior commissure (AC), a major

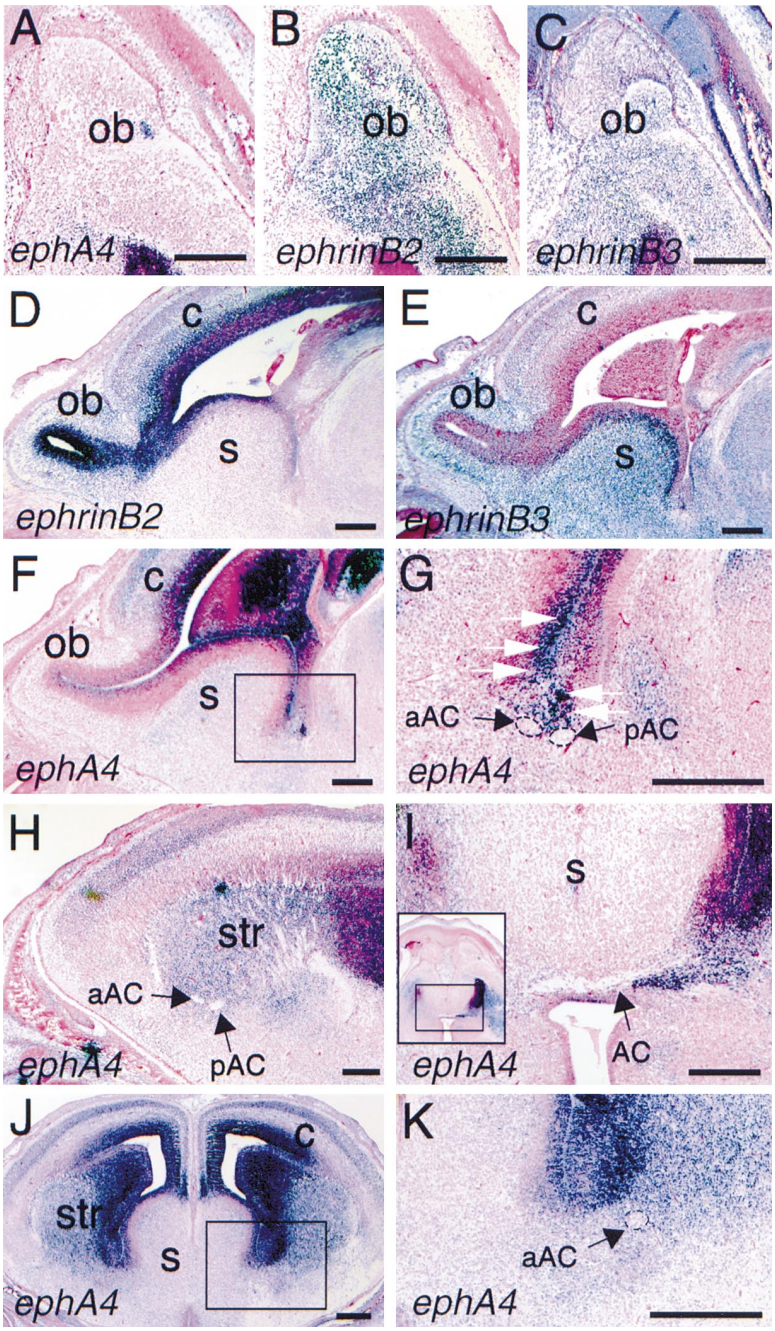

Figure 6. EphA4, EphrinB2, and EphrinB3 Expression in the Developing Forebrain

DIG in situ hybridizations (blue staining) on (A–C and I) horizontal sections of olfactory bulbs (anterior is top) (D–G) midsagittal (anterior is left), and (H) parasagittal sections of E15.5 mouse forebrain using the indicated antisense cRNA probes. Note expression of ephrinB2 and ephrinB3 mRNA in the developing olfactory bulb from where the anterior commissure (AC) fibers originate (B and C). Sagittal sections (D and E) show the complementary dorsal–ventral expression of ephrinB2 and eprinB3 mRNA. Strong ephA4 expression was seen in the ventricular zones (white arrows) and weaker expression is detected in the developing medial septum (s). (G) Higher magnification of (F) showing the transversely sectioned AC fibers (outlined by stippled line, black arrows) crossing the midline just ventral and in close contact with ephA4-expressing cells (white arrows). (H) In parasagittal sections, ephA4 mRNA was detected in the developing striatum (str) dorsal of the developing AC. (I) Oblique horizontal section at the level of the AC with the left side more ventral than the right side (inset shows position in forebrain). Few ephA4-positive cells were seen ventral of the aAC (left side), whereas strong ephA4 staining was detected dorsal and posterior of the aAC (right side; arrow). (K) Higher magnification of (J) showing ephA4 mRNA on a coronal section. Arrow points to the anterior AC positioned just ventral of strong ephA4 mRNA expression. Scale bars are 350 μm.

forebrain axon tract that consists of an anterior (aAC) and posterior branch (pAC), which connect both lobes of olfactory bulbs and temporal cortex, respectively (Dottori et al., 1998). The expression of EphA4 in developing forebrain was, however, not reported, and the contribution of EphA4 kinase signaling remained unclear (Dottori et al., 1998). By in situ hybridization analysis of E15.5 wild-type embryos, ephA4 mRNA appeared absent from developing olfactory bulbs (OB), which contain the cell bodies of neurons that form the aAC branch (Figures 6A and 6F). Conversely, ephrinB2 was specifically and strongly expressed by the majority of the cells in the OB (Figures 6B and 6D). EphrinB3 showed a more widespread expression pattern in the ventral forebrain that partially overlapped with ephrinB2 and included the OB (Figures 6C and 6E). These findings suggested that neurons of the OB express ephrinB ligands rather than EphA4. Consistent with these mRNA expression patterns, ephrinB proteins were previously found on aAC and pAC axons (Henkemeyer et al., 1996). In contrast, low levels of EphA4 expression were detected in the pAC but not in the aAC branch (Leighton et al., 2001). Rather, ephA4-positive cells were found dorsal of both branches of the anterior commissure, in the ventricular zone of the third ventricle and throughout the striatum (Figures 6F–6K). Of potential importance was the finding that cells strongly positive for the ephA4 probe were located immediately adjacent to AC axons (Figures 6G and 6K). In horizontal sections, ephA4-positive cells were found outlining the path of AC axons from the

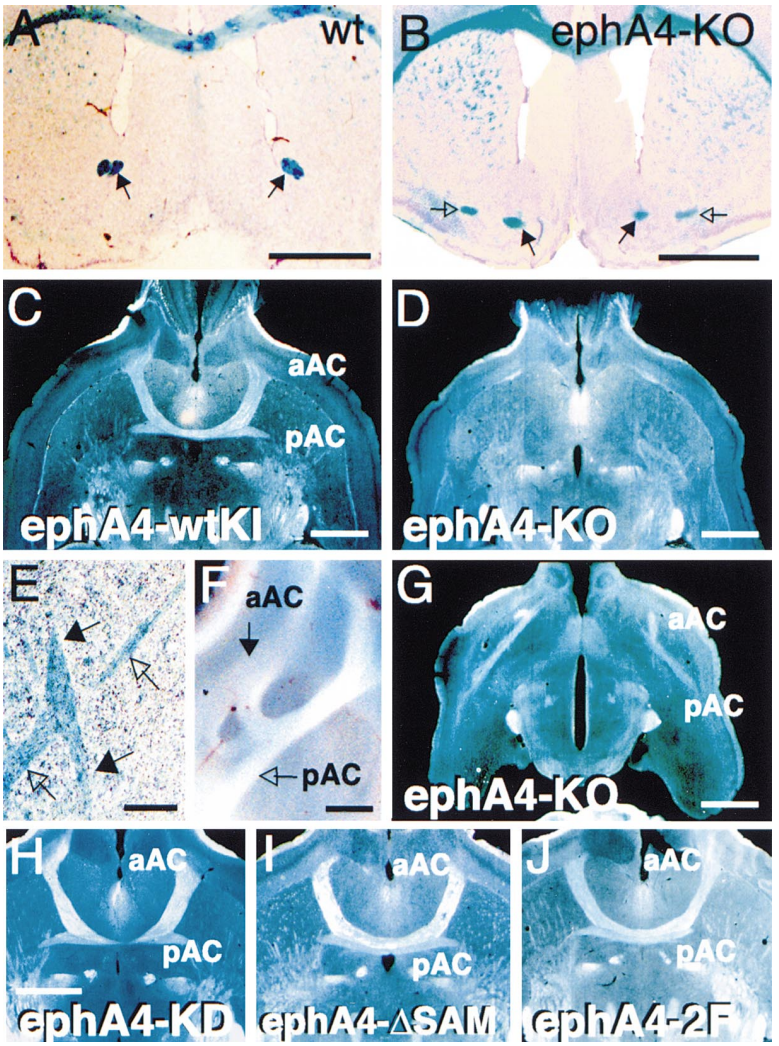

Figure 7. Rescue of Anterior Commissure (AC) Defect by Kinase-Dead and Signaling-Deficient EphA4 Mutants

(A and B) Coronal sections of 10-week-old wild-type (wt) and homozygous ephA4^{KO} brains stained with Luxol fast blue. In wt mice (A), aAC (black arrow) and pAC fibers (white arrow) were located just ventral of the third ventricles. In ephA4^{KO} mice (B), both aAC and pAC fibers were severely reduced and migrated much deeper into the ventral forebrain than in wt mice.

(C, D, and H–J) Dark-field micrographs of unstained horizontal sections at the level of the AC from 10-week-old forebrains of the indicated mutants. Both aAC and pAC limbs of the AC developed normally in homozygous (C) control *ephA4*^{wtKI}, (H) kinase-dead *ephA4*^{KD}, (I) *ephA4*$^{\Delta SAM}$, and (J) *ephA4*^{2F} mice. In contrast, the AC did not form in its normal location in (D) *ephA4*^{KO} mice.

(E–G) Luxol fast blue (E) and unstained (F and G) dark-field micrographs of homozygous *ephA4*^{KO} mice showing (E) aberrant crossing of aAC (black arrows) and pAC limbs (white arrows) on left side of the forebrain, thereby failing to cross the midline, and (F) aberrant U-turn of aAC into ipsilateral olfactory bulb after fasciculating with the pAC branch. (G) Section taken 300 μm ventral of section shown in D illustrates another example of the misprojected AC tracts.

Scale bars are 2 mm in (A)–(D) and (G)–(J); 500 μm in (E) and (F).

periphery to the midline during and shortly after AC tract formation (Figure 6I). These findings suggested a potential interaction between EphA4-positive cells adjacent to AC axons and ephrinB-expressing AC axons.

A Kinase-Independent Role for EphA4 in Anterior Commissure Formation

We next analyzed the morphology of the anterior commissure in adult *ephA4* mutant brains. Coronal sections of wild-type and homozygous control *ephA4*^{wtKI} mice showed the normal trajectory of AC axons just below the ventricular zone of the third ventricle and close to the ventral edge of the striatum (Figure 7A and data not shown). In contrast, in homozygous *ephA4* null mutants both branches of the AC were reduced in diameter and shifted ventrally, away from third ventricle and striatum (Figure 7B). Horizontal brain sections of homozygous control *ephA4*^{wtKI} mice and mice expressing signaling competent *ephA4*$^{\Delta SAM}$ receptors showed the normal horseshoe shaped aAC branches and the medial aspects of the normally formed pAC branches (Figures 7C and 7I; n = 4 of each genotype). In contrast and consistent with earlier findings (Dottori et al., 1998), *ephA4* null mutants showed agenesis of the AC with high penetrance (7 out of 13 analyzed; Figure 7D). In 6 of the affected cases, both branches of the AC failed to cross the midline (Figure 7G), whereas in one case, the left side of the AC was defective and the opposite AC unilaterally crossed the midline but failed to progress further (data not shown). Generally, aAC and pAC branches did not change their migration pattern when encountering the other branch suggesting that the component axons were not attracted to each other (Figure 7E). In one case, however, the aAC tracts fused with the pAC tracts and performed aberrant U-turns toward the ipsilateral olfactory bulb (Figure 7F). Interestingly, formation of the AC was completely rescued by kinase-dead *ephA4*^{KD} (n = 6) and the severe signaling mutant *ephA4*^{2F} (n = 8) (Figures 7H and 7J). These results demonstrate that EphA4 has kinase-independent functions in the formation of the AC.

Discussion

Here we show that EphA4 mediates the formation of axon tracts in the developing nervous system via two different mechanisms: (1) In the corticospinal tract, EphA4 is expressed on CST axons and prevents them

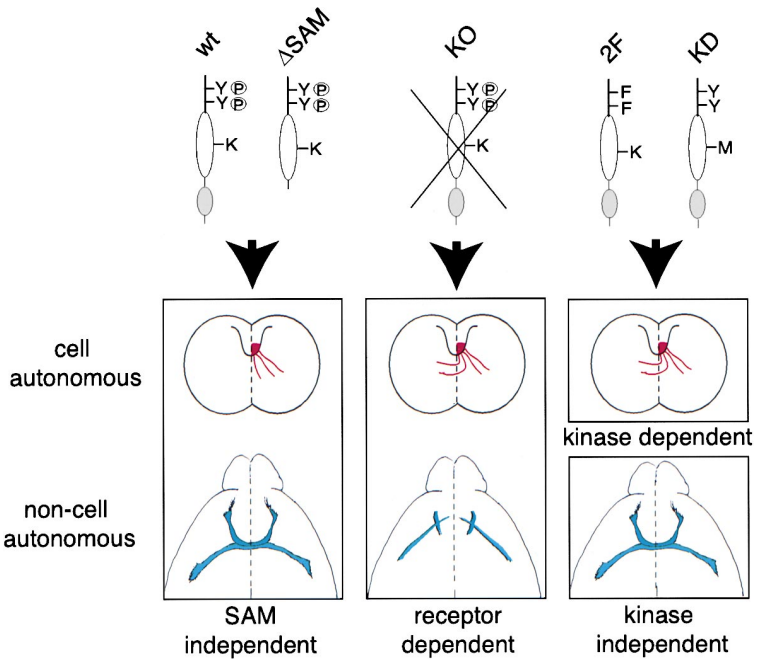

Figure 8. Model of EphA4 Signaling in Corticospinal Tract and Anterior Commissure Formation

Left side: EphA4 signals in CST axons via its intrinsic kinase activity, but not requiring its SAM domain, in a cell autonomous fashion to prevent them from recrossing the midline. In contrast, EphA4 mediates the formation of the AC in a non-cell-autonomous manner. Also, the formation of the AC is SAM independent.

Middle: Removal of EphA4 protein (in the null mutants) causes aberrant recrossing of CST axons and partially penetrant agenesis of the AC.

Right side: Kinase-dead or signaling-deficient mutants of EphA4 are unable to execute their normal guidance role in CST axons but completely rescue the AC phenotype.

from recrossing the midline in the spinal cord and brainstem. A catalytically active EphA4 kinase domain is required for normal CST formation and normal hindlimb motor coordination. These findings indicate that EphA4 acts as the signaling receptor for an ephrin ligand. A candidate ligand is ephrinB3, which is expressed in the spinal cord midline and whose removal by gene knockout experiments phenocopies the signaling-deficient *ephA4*^{KD} or *ephA4*^{2F} mutants (Yokoyama et al., 2001 [this issue of *Neuron*]; N. Gale, K. K., S. D. Croll, L. Pan, J. McClain, V. Hughes, S. Zabski, T. M. DeChiara, R. K., G. Yancopoulos, submitted). (2) EphA4 is also required for the formation of the anterior commissure. Unlike the situation in the CST, EphA4 expression is absent from aAC axons and high in cells adjacent to the developing AC tract. Moreover, an active kinase domain of EphA4 is not required, since AC formation is rescued in signaling-deficient *ephA4*^{KD} or *ephA4*^{2F} mutants. Thus, EphA4 mediates the formation of major axon tracts in both kinase-dependent and kinase-independent manner (Figure 8).

Although it is possible that in the anterior forebrain EphA4 mediates signals, which are independent of tyrosine phosphorylation, e.g., via PDZ domain effectors (Torres et al., 1998), we favor the notion that EphA4 acts as a "ligand" for ephrins which engage in "reverse" signaling. Since *ephrinB3* null mutants do not have defects in AC formation (N. Gale, K. K., S. D. Croll, L. Pan, J. McClain, V. Hughes, S. Zabski, T. M. DeChiara, R. K., G. Yancopoulos, submitted), ephrinB2 appears to be a likely candidate for this function. Unfortunately, *ephrinB2* null mutants die from an early vascular defect (Wang et al., 1998; Adams et al., 1999), and genetic proof for this hypothesis will have to await the generation of a nervous system–specific knockout of ephrinB2. Interestingly, targeted knockin of a carboxy-terminally truncated version of ephrinB2 leads to the same early vascular defect as in *ephrinB2* null mutants, suggesting a requirement for ephrinB2 reverse signaling in the developing vasculature (Adams et al., 2001). EphrinA ligands may also be mediators of kinase-independent functions of EphA4, since reverse signaling of ephrinA ligands has recently been suggested (Davy et al., 1999).

A rather surprising finding was that the EphA4 SAM domain was not required for identified kinase-dependent or kinase-independent functions of EphA4. SAM domains are highly conserved, independently folded modules in the cytoplasmic domain of all Eph receptors and not present in any other receptor tyrosine kinase (Schultz et al., 1997). Because SAM domains of EphA4 and EphB2 receptors can form dimers and oligomers (Smalla et al., 1999; Stapleton et al., 1999; Thanos et al., 1999), it was proposed that the SAM domain participates in or mediates the formation of higher order receptor aggregates, a prerequisite for full receptor signaling (Stein et al., 1998). Instead, our findings suggest that SAM domains are not required for EphA4-mediated axon guidance, neither for EphA4 kinase signaling, nor for clustering and ligand activation (assuming that kinase-independent functions are mediated by ephrin reverse signaling) (Figure 8). Whether SAM domains are important for Eph functions in cell migration or boundary formation remains to be established. Loss of the SAM domain may partially be compensated by interactions of the EphA4 carboxyl terminus with PDZ domain proteins, which can also serve to cluster membrane proteins (Sheng and Pak 2000). Therefore, targeted knockins of EphA4 mutants either lacking only the PDZ target site or both SAM domain and PDZ target site are being generated to address this possibility.

We herein show that the control of CST midline recrossing in the spinal cord is regulated by EphA4 kinase activity. Most likely, the corresponding ligand activating EphA4 to prevent aberrant midline recrossing is EphrinB3. How then can the CST axons cross the midline in the first place? Two alternative explanations are at hand. Either EphA4 is present on the CST axons only

after crossing the midline in the medulla or the expression of ephrinB3 is confined to the dorsal part of the midline at the time of crossing. We favor the latter explanation since it would involve less complicated temporal regulation of gene expression. What is the cause of the shallower dorsal funiculus in the EphA4 null and EphA4 kinase-deficient mice? While the shallower dorsal funiculus could be partly due to degeneration of misprojected CST axons, we cannot exclude the possibility that other defects in the spinal cord are responsible for the shift of the dorsal funiculus. Our preliminary data indicate a shallower dorsal funiculus already at P0, when the CST fibers have not yet reached the spinal cord. Future studies will provide answers to these and other questions regarding the role of EphA4 and its ligands in the spinal cord.

The EphA4 function in AC formation resembled in some ways the role of EphB2 in this structure. Both receptors are required for AC formation and exert their function in a non-cell-autonomous, kinase-independent fashion in cells adjacent to the axon tract. However, there are some interesting differences. EphB2 is only required for the posterior branch, whereas lack of EphA4 affected the formation of both aAC and pAC branches. EphB2 expression is predominant in cells ventral to the pAC, a domain that is normally avoided by pAC axons unless EphB2 expression is lost. Therefore, it was concluded that EphB2 mediates a repulsive signal for AC axons (Henkemeyer et al., 1996; Orioli et al., 1996). Here, we show that EphA4-positive cells are located primarily dorsal to the AC tract in the ventricular zone of the third ventricle and in striatum (see Figure 4). In the absence of EphA4, AC axons do not enter the EphA4 expression domain, but their projections are rather shifted ventrally away from EphA4-expressing cells. This phenotype suggests that EphA4 is an attractive/adhesive, rather than a repulsive cue for AC axons and that its mechanism of action is different from the related EphB2 receptor. One of the possible differences between EphA4 and EphB2 is that EphB2 interacts with both ephrinB1 and ephrinB2 on AC axons, whereas EphA4 only interacts with ephrinB2 and possibly with ephrinA ligands. Double *ephB2* and *ephA4* null mutants are being generated to investigate genetic interactions and cooperative guidance between these two receptors.

Experimental Procedures

Targeting Vectors, Southern Hybridization, and Generation of Mutant Mice

A replacement-type targeting construct for *ephA4* was generated by fusion of the wt ephA4 cDNA in frame to exon III in the 5.5 kb long arm of the vector via an Eco47III restriction site. A poly(A) tail, a PGK-driven *neo* cassette flanked by loxP sites and a 1.2 kb short arm completed the construct at the 3′ site. Into this targeting construct we placed cDNAs encoding either wild-type (ephA4^{wtKI}) or various mutants of mouse EphA4. The *ephA4*$^{\Delta SAM}$ allele encoded EphA4 with the entire SAM domain deleted, encompassing amino acid (aa) residues 905–974 (PEF…MRT), leaving the 12 last aa residues intact. The *ephA4*^{2F} allele encoded EphA4 with the two juxtamembrane tyrosine residues Y596 and Y602 replaced with phenylalanines. The kinase-dead *ephA4*^{KD} allele encoded EphA4 with lysine K653 replaced with a methionine. Mutated cDNAs were produced by site-directed mutagenesis using high-fidelity polymerases in PCR reactions according to standard protocols and were subsequently sequenced to verify correct mutations. Gene targeting by homologous recombination in E14.1 ES cells was done according to standard protocols. BamHI-digested DNA from positive clones was used for Southern hybridization with a 800 bp XhoI–ApaI fragment (3′ probe), located adjacent to the 3′ end of the recombination region. After blastocyst injection, generation of chimeric mice, and backcrossing to C57BL/6 wild-type animals, one line for each cDNA insertion, ephA4^{wtKI}, ephA4$^{\Delta SAM}$, ephA4^{2F}, and ephA4^{KD} was established successfully. The loxP flanked *neo* cassette was removed in vivo by crossbreeding to a Cre recombinase expressing transgenic mouse strain (Schwenk et al., 1995), followed by backcrossing to wild-type animals (both in C57BL/6 background). Absence of *neo* was identified by PCR on genomic DNA from tail biopsies. Animals without *Cre* or in control experiments using ephA4^{2F} mice without *neo* and *Cre* alleles were used for phenotypic analysis described in this study. Mutant phenotypes were analyzed in comparable mixed 129/svev × C57BL/6 backgrounds for *ephA4*^{wtKI}, *ephA4*^{dSAM}, *ephA4*^{2F}, and *ephA4*^{KD} mice. Tissue from embryonic yolk sacs or tail biopsies was used for PCR genotyping of animals.

Wheat Germ Agglutinin Pull-Down, Immunoprecipitation, and Western Blotting

Brains from adult wild-type or *ephA4* mutant mice were quickly dissected and homogenized in cold lysis buffer (50 mM Tris/HCl [pH 7.5], 120 mM NaCl, 1% Triton X-100, 1 mM sodium orthovanadate, 1× complete protease inhibitor cocktail [Roche]). Glycosylated proteins were enriched by pull-down with sepharose-coupled Triticum vulgaris lectin (Sigma, L6257). For neuronal cultures, cerebral cortices were dissected from E15.5 mouse embryos derived from intercrosses of either wild-type or heterozygote/homozygote intercrosses of ephA4^{2F} or ephA4^{KO} mice. Cortical neurons were dissociated and plated onto poly-L-lysine hydrobromide (Sigma) in the presence of 10% heat-inactivated horse serum for 3 hr. Cultures were maintained in N2-MEM medium (de Hoop et al., 1998) for 16 hr at 37°C in 5% carbon dioxide for starvation. After genotyping of yolk sacs, cultures were stimulated for 10 min with ephrinB3-IgG Fc fusion protein (R&D Systems, 1.0 μg/ml) clustered by preincubation (30 min) with a goat anti-human IgG-specific antibody (Jackson Laboratories, 0.2 μg antibody/μg fusion protein). For EphA4 overexpression experiments, constructs for ephA4^{WT}, ephA4$^{\Delta SAM}$, ephA4^{2F}, ephA4^{KD}, ephA4$^{KD/\Delta SAM}$, or empty vector (mock) were transfected into HEK293 cells using the calcium phosphate method and incubated for 48 hr to allow for gene expression. Cortical cultures or HEK293 cells were harvested in 1 ml lysis buffer and lysates were cleared by centrifugation for 30 min at 15,000 rpm, 4°C. EphA4 receptors were immunoprecipitated (IP) from the supernatants with a rabbit anti-EphA4 antiserum (Martone et al., 1997) and protein A sepharose CL-4B beads (Amersham) for an additional 2 hr at 4°C. For the GST pull-down experiments, HEK293 cell lysates were incubated with GST fusion proteins previously coupled to glutathion beads. We used GST proteins fused to the C-terminal SH2 domain of PLC-γ, the SH2 domain of pp60^{Src}, the SH2 domain of the p85 subunit of PI3K, the full-length Grb2 protein (Ponzetto et al., 1994), and the SH2 domain of Grb10 (Ooi et al., 1995). Incubations were for 4–5 hr at 4°C in the presence of 1 mM sodium vanadate and 2 mM DTT. After washing of IPs or GST pull-downs in lysis buffer, samples were analyzed by SDS–PAGE/immunoblotting with antibodies specific for EphA4, phosphotyrosine (Upstate Biotechnology, clone 4g10), and developed using secondary HRP-coupled antibodies and ECL Detection Reagent (Amersham).

EphA4 In Vitro Kinase Assays

IPs prepared as described above were washed three times with lysis buffer and two times with kinase buffer (20 mM HEPES [pH 7.5], 10 mM $MnCl_2$, 1 mM DTT, 0.1% NP-40, 1 mM sodium vanadate, and 5 μM ATP). Kinase assays were performed in 20 μl of kinase buffer, 4 μM enolase (Sigma), prepared as previously described (Courtneidge et al., 1993), and 5 μCi of ^{32}P-γ-ATP for 10 min at 30°C. The samples were analyzed by 7.5% SDS–PAGE and phosphoproteins visualized by autoradiography.

Tracing of the Corticospinal Tract

Animals were anesthetized with a ketamine/xylacine mix (100/10 mg/kg body weight; i.p., Ketalar, Parke-Davis) and the motor cortex

was pressure injected with the anterograde tracer biotin dextrane amine (10% BDA in 0.1 M phosphate buffer (PB); Molecular Probes; 4 μl into eight to ten injection sites). After a survival time of 10–14 days, the animals were killed by an overdose of ketamine/xylacine and perfused transcardially with 0.1 M phosphate buffered saline (PBS) at pH 7.4, followed by 4% paraformaldehyde in PBS. Brain and spinal cord were dissected, postfixed in 4% PFA for 2 hr at 4°C, and stored in a 30% sucrose solution for 24 hr at 4°C for cryoprotection. Samples were embedded in Tissue Tek (Sakura Finetechnical) and frozen by placement of the cryomold directly on dry ice. Cryosections (50–100 μm) were collected in cold 0.1 M PB, rinsed 3 × 30 min in PBS plus 0.1% Triton X-100 (PBT) and incubated overnight with an avidin-biotin-peroxidase complex (Vectastain ABC Elite Kit, 1:100 in PBT) at room temperature. After 3 × 30 min washing in PBT, the sections were rinsed with 50 mM Tris-HCl (pH 8.0) and reacted with a DAB-peroxidase staining kit (Vector Burlingame). After 10–30 min, the reaction was stopped with 50 mM Tris-HCl, and the sections were rinsed 3 × 10 min in 50 mM Tris-HCl. Sections were mounted on slides, dehydrated, cleared in a 1:1 mixture of benzyl alcohol/benzyl bensoate (BABB), cover slipped, and examined under darkfield optics using a Zeiss Axiophot microscope.

Tissue Processing

Spinal cords or brains from perfused animals were dissected, postfixed in 4% PFA, cryoprotected, and embedded in Tissue Tek. For gray matter stain, spinal cord cryosections (50–100 μm) were incubated 24 hr in DAB solution from a DAB-peroxidase staining kit to reveal endogenous peroxidase activity in cell bodies. For myelin stain of the AC (Kluver and Barrera, 1953), 20 μm cryostat brain sections were collected on glass slides, dried, and dehydrated. The slides were incubated for 5 hr at 60°C in 0.1% luxol fast blue (LXFB MBS #34044, BDH Laboratory Supplies) solution (95% ethanol, 0.5% acetic acid), washed in 95% ethanol, followed by a wash in distilled water. Differentiation was initiated by immersion for 10 s in 0.05% lithium carbonate and completed by immersion for 30–60 s in 70% ethanol. After repeating differentiation until desired stain was achieved, slides were rinsed in distilled water, counterstained with cresyl violet, and mounted. For detection of the AC in brains of mutant mice, 30–100 μm cryostat floating sections were collected in PBS, mounted on slides, and photographed while wet using a Nikon SMZ-U dissecting microscope equipped with a subilluminating module. PLAP stains were done according to Leighton et al. (2001).

In Situ Hybridization

DIG in situ hybridizations on 8 μm paraffin sections of E15.5 embryo heads or P4 spinal cords were performed according to standard protocols. Antisense riboprobes were transcribed in vitro and labeled by incorporation of digoxygenin-linked UTP (Roche) from the following linearized templates: *ephrinB2*, a 890 bp fragment extending from nucleotide 4–894 (accession number U16819); *ephrinB3*, a 1021 bp fragment extending from nucleotide 1–1021 (accession number NM007911); *ephA4*, a 1551 bp fragment extending from nucleotide 1–1551 (accession number NM007936).

Acknowledgments

We gratefully acknowledge Marc Tessier-Lavigne and Philip A. Leighton for sharing unpublished data and for providing panel (D) of Figure 5. We thank K. Vintersten of the Transgenic Service and staff of EMBL Laboratory Animal Resources for generation of chimeric mice and expert support, J. Jackson for help with tracings, D. Panayi and D. Young for help with video clips. EphA4 antiserum, GST Grb-10, kinase-dead ephA4, and IgG Fc were generous gifts from E. Pasquale, B. Margolis, D. Wilkinson, and Regeneron, Inc., respectively. G. A. Wilkinson, R. H. Adams, J. Taylor are acknowledged for critically reading the manuscript. Support for this study came in part from the Leukaemia Foundation of Queensland (A. W. B.), the Deutsche Forschungsgemeinschaft (SFB 488 and KL948/4 to R. K.), from Human Frontiers Science Program Organization, and TMR grants to R. K. and K. K., respectively. K. K. is a Marie Curie Fellow.

Received October 18, 2000; revised November 17, 2000.

References

Adams, R.H., Wilkinson, G.A., Weiss, C., Diella, F., Gale, N.W., Deutsch, U., Risau, W., and Klein, R. (1999). Roles of ephrinB ligands and EphB receptors in cardiovascular development: demarcation of arterial/venous domains, vascular morphogenesis and sprouting angiogenesis. Genes Dev. *13*, 295–306.

Adams, R.H., Diella, F., Hennig, S., Helmbacher, F., Deutsch, U., and Klein, R. (2001). The cytoplasmic domain of the ligand ephrinB2 is required for vascular morphogenesis but not cranial neural crest migration. Cell *104*, 57–69.

Binns, K.L., Taylor, P.P., Sicheri, F., Pawson, T., and Holland, S.J. (2000). Phosphorylation of tyrosine residues in the kinase domain and juxtamembrane region regulates the biological and catalytic activities of Eph receptors. Mol. Cell. Biol. *20*, 4791–4801.

Birgbauer, E., Cowan, C.A., Sretavan, D.W., and Henkemeyer, M. (2000). Kinase independent function of EphB receptors in retinal axon pathfinding to the optic disc from dorsal but not ventral retina. Development *127*, 1231–1241.

Brown, A., Yates, P.A., Burrola, P., Ortuno, D., Vaidya, A., Jessell, T.M., Pfaff, S.L., O'Leary, D.D.M., and Lemke, G. (2000). Topographic mapping from the retina to the midbrain is controlled by relative but not absolute levels of EphA receptor signaling. Cell *102*, 77–88.

Brückner, K., and Klein, R. (1998). Signaling by Eph receptors and their ephrin ligands. Curr. Opin. Neurobiol. *8*, 375–382.

Brückner, K., Pasquale, E.B., and Klein, R. (1997). Tyrosine phosphorylation of transmembrane ligands for Eph receptors. Science *275*, 1640–1643.

Brückner, K., Labrador, J.P., Scheiffele, P., Herb, A., Bradke, F., Seeburg, P.H., and Klein, R. (1999). EphrinB ligands recruit GRIP family PDZ adaptor proteins into raft membrane microdomains. Neuron *22*, 511–524.

Buchert, M., Schneider, S., Meskenaite, V., Adams, M.T., Canaani, E., Baechi, T., Moelling, K., and Hovens, C.M. (1999). The junction-associated protein AF-6 interacts and clusters with specific Eph receptor tyrosine kinases at specialized sites of cell-cell contact in the brain. J. Cell Biol. *144*, 361–371.

Chin-Sang, I.D., George, S.E., Ding, M., Modeley, S.L., Lynch, A.S., and Chisholm, A.D. (1999). The ephrin VAB-2/EFN-1 functions in neuronal signaling to regulate epidermal morphogenesis in *C. elegans*. Cell *99*, 781–790.

Courtneidge, S.A., Dhand, R., Pilat, D., Twamley, G.M., Waterfield, M.D., and Roussel, M.F. (1993). Activation of Src family kinases by colony stimulating factor-1, and their association with its receptor. EMBO J. *12*, 943–950.

Cowan, C.A., Yokoyama, N., Bianchi, L.M., Henkemeyer, M., and Fritzsch, B. (2000). EphB2 guides axons at the midline and is necessary for normal vestibular function. Neuron *26*, 417–430.

Davy, A., Gale, N.W., Murray, E.W., Klinghoffer, R.A., Soriano, P., Feuerstein, C., and Robbins, S.M. (1999). Compartmentalized signaling by GPI-anchored ephrin-A5 requires the Fyn tyrosine kinase to regulate cellular adhesion. Genes Dev. *13*, 3125–3135.

de Hoop, M.J., Meyn, L., and Dotti, C.G. (1998). Culturing hippocampal neurons and astrocytes from fetal rodent brain. In Cell Biology, Second Edition, J.E. Celis, ed. (Denmark: University of Aahus), 154–163.

Dottori, M., Hartley, L., Galea, M., Paxinos, G., Polizzotto, M., Kilpatrick, T., Bartlett, P.F., Murphy, M., Köntgen, F., and Boyd, A.W. (1998). EphA4 (Sek1) receptor tyrosine kinase is required for the development of the corticospinal tract. Proc. Natl. Acad. Sci. USA *95*, 13248–13253.

Feldheim, D.A., Kim, Y.I., Bergemann, A.D., Frisen, J., Barbacid, M., and Flanagan, J.G. (2000). Genetic analysis of ephrin-A2 and ephrin-A5 shows their requirement in multiple aspects of retinocollicular mapping. Neuron *25*, 563–574.

Feng, G., Laskowski, M.B., Feldheim, D.A., Wang, H., Lewis, R., Frisen, J., Flanagan, J.G., and Sanes, J.R. (2000). Roles for ephrins in positionally selective synaptogenesis between motor neurons and muscle fibers. Neuron *25*, 295–306.

Flanagan, J.G., and Vanderhaeghen, P. (1998). The ephrins and Eph receptors in neural development. Annu. Rev. Neurosci. *21*, 309–345.

Gale, N.W., Holland, S.J., Valenzuela, D.M., Flenniken, A., Pan, L., Ryan, T.E., Henkemeyer, M., Strebhardt, K., Hirai, H., Wilkinson, D.G., et al. (1996). Eph receptors and ligands comprise two major specificity subclasses, and are reciprocally compartmentalized during embryogenesis. Neuron *17*, 9–19.

Gerety, S.S., Wang, H.U., Chen, Z.F., and Anderson, D.J. (1999). Symmetrical mutant phenotypes of the receptor EphB4 and its specific transmembrane ligand ephrinB2 in cardiovascular development. Mol. Cell *4*, 403–414.

Helmbacher, F., Schneider-Maunoury, S., Topilko, P., Tiret, L., and Charnay, P. (2000). Targeting of the EphA4 tyrosine kinase receptor affects dorsal/ventral pathfinding of limb motor axons. Development *127*, 3313–3324.

Henkemeyer, M., Orioli, D., Henderson, J.T., Saxton, T.M., Roder, J., Pawson, T., and Klein, R. (1996). Nuk controls pathfinding of commissural axons in the mammalian central nervous sustem. Cell *86*, 35–46.

Hock, B., Böhme, B., Karn, T., Yamamoto, T., Kaibuchi, K., Holtrich, U., Holland, S., Pawson, T., Rübsamen-Waigmann, H., and Strebhardt, K. (1998). PDZ-domain-mediated interaction of the Eph-related receptor tyrosine kinase EphB3 and the ras-binding protein AF6 depends on the kinase activity of the receptor. Proc. Natl. Acad. Sci. USA *95*, 9779–9784.

Holder, N., and Klein, R. (1999). Eph receptors and ephrins: effectors of morphogenesis. Development *126*, 2033–2044.

Holland, S.J., Gale, N.W., Mbamalu, G., Yancopoulos, G.D., Henkemeyer, M., and Pawson, T. (1996). Bidirectional signaling through the EPH-family receptor Nuk and its transmembrane ligands. Nature *383*, 722–725.

Holland, S.J., Peles, E., Pawson, T., and Schlessinger, J. (1998). Cell-contact-dependent signaling in axon growth and guidance: Eph receptor tyrosine kinases and receptor protein tyrosine phosphatases β. Curr. Opin. Neurobiol. *8*, 117–127.

Hornberger, M.R., Dutting, D., Ciossek, T., Yamada, T., Handwerker, C., Lang, S., Weth, F., Huf, J., Wessel, R., Logan, C., et al., (1999). Modulation of EphA receptor function by coexpressed ephrinA ligands on retinal ganglion cell axons. Neuron *22*, 731–742.

Imondi, R., Wideman, C., and Kaprielian, Z. (2000). Complementary expression of transmembrane ephrins and their receptors in the mouse spinal cord: a possible role in constraining the orientation of longitudinally projecting axons. Development *127*, 1397–1410.

Joosten, E.A.J., and Bär, D.P.R. (1999). Axon guidance of outgrowing corticospinal fibres in the rat. J. Anat. *194*, 15–32.

Kalo, M.S., and Pasquale, E.B. (1999). Signal transfer by Eph receptors. Cell Tissue Res. *298*, 1–9.

Klein, R. (1999). Bi-directional signals establish boundaries. Curr. Biol. *9*, R691–R694.

Kluver, H., and Barrera, E. (1953). A method for the combined staining of cells and fibers in the nervous system. J. Neuropath. Exp. Neurol. *12*, 400–403.

Leighton, P.A., Mitchell, K.J., Goodrich, L., Lu, X., Pinson, K., Wakenight, P., Tate, P., Skarnes, W.C., and Tessier-Lavigne, M. (2001). A large scale gene trap screen for brain wiring molecules in mice. Nature, in press.

Lin, D., Gish, G.D., Songyang, Z., and Pawson, T. (1999). The carboxyl terminus of B class ephrins constitutes a PDZ domain binding motif. J. Biol. Chem. *274*, 3726–3733.

Martone, M.E., Holash, J.A., Bayardo, A., Pasquale, E.B., and Ellisman, M.H. (1997). Immunolocalization of the receptor tyrosine kinase EphA4 in the adult rat central nervous system. Brain Res. *771*, 238–250.

Mellitzer, G., Xu, Q., and Wilkinson, D.G. (1999). Eph receptors and ephrins restrict cell intermingling and communication. Nature *400*, 77–81.

O'Leary, D.D.M., and Wilkinson, D.G. (1999). Eph receptors and ephrins in neural development. Curr. Opin. Neurobiol. *9*, 65–73.

Ooi, J., Yajnik, V., Immanuel, D., Gordon, M., Moskow, J.J., Buchberg, A.M., and Margolis, B. (1995). The cloning of Grb10 reveals a new family of SH2 domain proteins. Oncogene *10*, 1621–1630.

Orioli, D., Henkemeyer, M., Lemke, G., Klein, R., and Pawson, T. (1996). Sek4 and Nuk receptors cooperate in guidance of commissural axons and in palate formation. EMBO J. *15*, 6035–6049.

Park, S., Frisen, J., and Barbacid, M. (1997). Aberrant axonal projections in mice lacking EphA8 (Eek) tyrosine protein kinase receptors. EMBO J. *16*, 3106–3114.

Ponzetto, C., Bardelli, A., Zhen, Z., Maina, F., dalla Zonca, P., Giordano, S., Graziani, A., Panayotou, G., and Comoglio, P.M. (1994). A multifunctional docking site mediates signaling and transformation by the hepatocyte growth factor/scatter factor receptor family. Cell *77*, 261–271.

Schultz, J., Ponting, C.P., Hofmann, K., and Bork, P. (1997). SAM as a protein interaction domain involved in developmental regulation. Protein Sci. *6*, 249–253.

Schwenk, F., Baron, U., and Rajewsky, K. (1995). A cre-transgenic mouse strain for the ubiquitous deletion of loxP-flanked gene segments including deletion in germ cells. Nucleic Acids Res. *23*, 5080–5081.

Sheng, M., and Pak, D.T. (2000). Ligand-gated ion channel interactions with cytoskeletal and signaling proteins. Annu. Rev. Physiol. *62*, 755–778.

Smalla, M., Schmieder, P., Kelly, M., Ter Laak, A., Krause, G., Ball, L., Wahl, M., Bork, P., and Oschkinat, H. (1999). Solution structure of the receptor tyrosine kinase EphB2 SAM domain and identification of two distinct homotypic interaction sites. Protein Sci. *8*, 1954–1961.

Stapleton, D., Balan, I., Pawson, T., and Sicheri, F. (1999). The crystal structure of an Eph receptor SAM domain reveals a mechanism for modular dimerization. Nat. Struct. Biol. *6*, 44–49.

Stein, E., Lane, A.A., Cerretti, D.P., Schoecklmann, H.O., Schroff, A.D., Van Etten, R.L., and Daniel, T.O. (1998). Eph receptors discriminate specific ligand oligomers to determine alternative signaling complexes, attachment, and assembly responses. Genes Dev. *12*, 667–678.

Thanos, C.D., Goodwill, K.E., and Bowie, J.U. (1999). Oligomeric structure of the human EphB2 receptor SAM domain. Science *283*, 833–836.

Torres, R., Firestein, B.L., Dong, H., Staudinger, J., Olson, E.N., Huganir, R.L., Bredt, D.S., Gale, N.W., and Yancopoulos, G.D. (1998). PDZ proteins bind, cluster and synaptically co-localize with Eph receptors and their ephrin ligands. Neuron *21*, 1453–1463.

Wang, H.U., Chen, Z.-F., and Anderson, D.J. (1998). Molecular distinction and angiogenic interaction between embryonic arteries and veins revealed by ephrin-B2 and its receptor Eph-B4. Cell *93*, 741–753.

Wang, X., Roy, P.J., Holland, S.J., Zhang, L.W., Culotti, J.G., and Pawson, T. (1999). Multiple ephrins control cell organization in C. elegans using kinase-dependent and -independent functions of the VAB-1 Eph receptor. Mol. Cell *4*, 903–913.

Wilkinson, D.G. (2000). Eph receptors and ephrins: regulators of guidance and assembly. Int. Rev. Cytol. *196*, 177–244.

Xu, Q., Mellitzer, G., Robinson, V., and Wilkinson, D.G. (1999). In vivo cell sorting in complementary segmental domains mediated by Eph receptors and ephrins. Nature *399*, 267–271.

Yokoyama, N., Romero, M.I., Cowan, C.A., Galvan, P., Helmbacher, F., Charnay, P., Parada, L.F., and Henkemeyer, M. (2001). Forward signaling mediated by ephrinB3 prevents contralateral corticospinal axons from recrossing the spinal cord midline. Neuron *29*, this issue, 85–97.

Zisch, A.H., Pazzagli, C., Freeman, A.L., Schneller, M., Hadman, M., Smith, J.W., Ruoslahti, E., and Pasquale, E.B. (2000). Replacing two conserved tyrosines of the EphB2 receptor with glutamic acid prevents binding of SH2 domains without abrogating kinase activity and biological responses. Oncogene *19*, 177–187.